ELSEVIER

Journal of Photochemistry and Photobiology A: Chemistry 89 (1995) 239–245

Journal of PHOTOCHEMISTRY AND PHOTOBIOLOGY A:CHEMISTRY

Quantitative binding and aggregation of R123 and R6G rhodamines at the surface of DPPG and DPPS phospholipid vesicles

Michel Deumié, Philippe Lorente, David Morizon

Laboratoire de Chimie Physique, Université de Perpignan, 52 avenue de Villeneuve, 66860 Perpignan Cedex, France

Received 21 December 1994; accepted 7 February 1995

Abstract

The ability of host molecules, such as vesicle-forming phospholipids, to alter significantly the spectroscopic behaviour of guest molecules was used to study the microenvironment and binding properties of two important dyes. The interaction and aggregation processes which occur between cationic dyes of the rhodamine family (R123 and R6G) and negatively charged vesicles of DL-a-dipalmitoylphosphatidyl-L-serine (DPPS) and L-a- dipalmitoylphosphatidyl-DL-glycerol (DPPG) phospholipids were used as a convenient scheme for the investigation of the electrostatic stabilization of biosystems. Fluorescence was used as a monitor for the processes of binding and aggregation of the cationic ligands on the vesicles in aqueous solution, and the phenomena were treated quantitatively using a resolution procedure of complex fluorescence spectra. Organized macrosystems of DPPG and DPPS vesicles obtained by sonication presented distinctive numbers of sites (n) for interaction with R123 and R6G dyes. Values of $n = 14$ (R123) and $n = 24$ (R6G) were obtained by titration with DPPS vesicles, while two kinds of sites were found with DPPG vesicles. The first class of sites ($n^a = 53$ (R123) and $n^a = 24$ (R6G)) was determined in the presence of low concentrations of DPPG vesicles; the second class of sites ($n^b = 36$ (R123) and $n^b = 6$ (R6G)) was found for larger concentrations of DPPG vesicles. These interactions involve reversible binding of the dyes to the vesicles in a multiple equilibria process well described by the identical and independent site model. At high vesicle concentrations, the quantitative binding vs. aggregation of the rhodamines at the surface of the vesicles can thus be seen as a disaggregation process; the rationale for these results is that esterified rhodamines in these heterogeneous solutions seek out electrostatic attraction and binding on the anionic head groups of the lipids with a definite number of sites.

Keywords: Rhodamines; Fluorescence; Phospholipid vesicles; Quantitative binding; Aggregation

1. Introduction

The selective biodistribution of an ionic drug in tissues and membranes [1] depends on its self-interacting properties (aggregation) and complex interactions with its molecular surroundings [2]. The importance of aggregation vs. individual binding has been widely recognized [3]. The formation of aggregates influences the photophysical properties of the dye molecule [4], while binding on uptake into a lipophilic environment results in an increase in its photosensitizing properties [5]. Significantly, the dyes show the same colour changes in the presence of charged colloids as in the presence of biological materials. Mataga and Koizumi [6] have shown that the change in the (S_0–S_1) spectra of organic dyestuffs brought about by the bonding of two rhodamine dyes with charged phospholipid vesicles can be explained only by a change in the dye aggregation in the S_0 state [7], so that the observed variations in S_0 can be equally monitored by absorption or fluorescence. Fluorometric investigations of bilayer phospholipid systems may thus provide an insight into the hydrophobic–electrostatic interactions and aggregation in membranes of the rhodamine probes R123 and R6G (Fig. 1) widely used in biological applications [8]. Although these dyes are positively charged at physiological pH, the charge is distributed over their aromatic rings and thus does

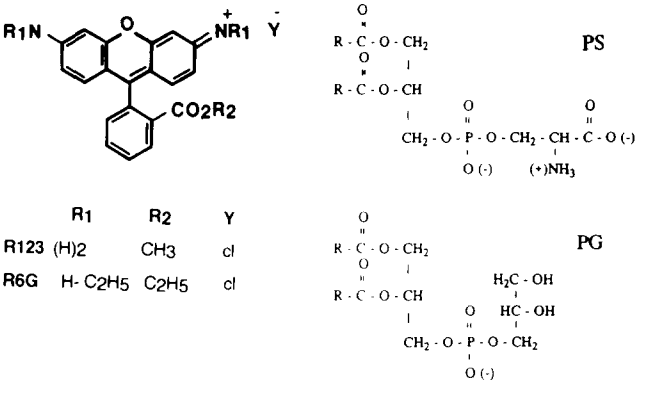

Fig. 1. R123 and R6G esterified rhodamines and the negatively charged phospholipids (PS, phosphatidylserine; PG, phosphatidylglycerol).

SDI 1010-6030(95)04058-7

not interfere with their lipophilic nature. Owing to the association of a large molecular size with considerable charge resonance characteristics of the lower energy states, the dipolar and highly polarizable R123 and R6G dyes tend to aggregate in solution [9]. Indeed, R123 and R6G molecules are amphipathic rather than lipophilic [10], and like many organic dyes [11] they usually show a change in their acid–base and optical properties in the presence of bilayer membranes of negative charge. Such spectral peculiarities have been observed in the behaviour of dye–surfactant systems carrying opposite charges [12], showing qualitatively that the net charges of dye and lipid molecules control most of their complex interactions and dependence [13].

Since these dyes are capable of interacting with mitochondrial receptors [14], biological applications of the rhodamine probes have received particular attention in the last decade [8]. However, not as much work has been done on the detailed quantitative analysis of their behaviour in simple model bilayers. In the equilibrium binding studies described in this paper, a fixed amount of a rhodamine dye (1.6×10^{-6} M) was titrated with increasing concentrations of sonicated lipid vesicle solution. Negatively charged vesicles of DL-a-dipalmitoylphosphatidyl-L-serine (DPPS) and L-a- dipalmitoylphosphatidyl-DL-glycerol (DPPG) (Fig. 1) were used to study the competitive coulombic–hydrophobic interactions [15] governing the lipid vesicle binding of the polar dye substrates. The extent of binding was monitored by the changes observed in the fluorescence wavelength and intensity, and a quantitative study of dye binding and aggregation at the surface of the vesicles was performed by fluorescence titration with spectral resolution of composite spectra.

2. Experimental details

2.1. Chemicals and apparatus

Rhodamine 123 chloride (R123) and rhodamine 6G chloride (R6G) were laser grade dyes bought from Molecular Probes. DPPS and DPPG lipids were obtained from Sigma. Water solutions were made from decarbonated and deionized water; all other solvents were of spectroquality grade from Fluka AG and did not show any spurious absorption or fluorescence. R123 and R6G exist in neutral water as fluorescent cationic forms whose emission maxima $\lambda_D{}^+$ are given in Table 1.

The instruments for recording the absorption, excitation and fluorescence spectra have been described previously [16]. The spectrofluorometer was interfaced with a Tandon AT 286 microcomputer for scanning the monochromators and recording the data. Experiments were conducted at 295 K in 1 or 0.5 cm (fluorescence) and 4 cm (absorption) quartz cuvettes. Excitation at 480 nm, unless otherwise specified, with excitation and emission slits of 4 nm, was chosen to

Table 1
The fluorescence maximum wavelengths of R123 and R6G rhodamines (1.6×10^{-6} M) measured in homogeneous solutions (water, octanol) and in the presence of DPPG and DPPS vesicles at typical lipid concentrations ([lipid]) and dye/vesicle ([D]/[ves]) concentration ratios. The subscript D^+ characterizes the free species in water or octanol; the subscript D_L or L refers to the situation in which rhodamine ligands are individually and independently bound to the lipid vesicles (at high [ves]); the subscript D_n (or agg) characterizes the particular situation in which the aggregation of the rhodamine ligands at the surface of the vesicles is at a maximum (low [ves])

		Water	DPPG	DPPS	Octanol
R123					
F_{D+}	λ_{D+} (nm)	528			538
F_{Dn}	λ_{Dn} (nm)		526 [b]	528	
	$[lipid]_{agg}$ (M)		3.2×10^{-5}	10^{-4}	
	$[D]/[ves]_{agg}$		150	48	
	n [a]		53	14	
F_{DL}	λ_{DL} (nm)		537	537	
	$[lipid]_L$ (M)		$>8\times10^{-4}$	$>5\times10^{-4}$	
	$[D]/[ves]_L$		<6	<10	
	n [a]		36	14	
R6G					
F_{D+}	λ_{D+} (nm)	550			560
F_{Dn}	λ_{Dn} (nm)		558 [b]	552	
	$[lipid]_{agg}$ (M)		2×10^{-5}	9×10^{-5}	
	$[D]/[ves]_{agg}$		240	53	
	n [a]		24	24	
F_{DL}	λ_{DL} (nm)		559	560	
	$[lipid]_L$ (M)		$>10^{-3}$	$>3.3\times10^{-4}$	
	$[D]/[ves]_L$		<5	<14	
	n [a]		6	24	

[a] Part of the results of Table 2 given here for comparison.
[b] Broad spectrum of low intensity.

avoid any reabsorption of the emitted light. Calibration curves and composite fluorescence spectra were obtained for varying lipid concentrations but fixed slit and sensitivity conditions.

2.2. Dye solutions and phospholipid vesicle preparation

As Beer's law was obeyed over the concentration range 10^{-7}–10^{-5} M, dye concentrations were held to a value of 1.6×10^{-6} M; the solutions were unbuffered and were not degassed (as oxygen inhibits the photodecomposition of rhodamines [17]). To combine an efficient excitation wavelength with a minimum inner filter effect [18], λ_{Exc} at 480 nm was selected. Such conditions mean that the reabsorption of the emitted light due to the overlap of the principal (S_0–S_1) excitation band, which may be important for these dyes which have small Stokes shifts [19] and large extinction coefficients, is negligible.

Small unilamellar solid phase vesicles from DPPS and DPPG were prepared according to described procedures [20]. A lipid solution (2 ml) in benzene was evaporated under vacuum. Deionized water was added to give the desired lipid concentration. The sample was sonicated at 295 K under a flow of N_2 using a Branson 250 sonifier II model at 1000 W for 15 min in 0.5 min intervals with a 1.27 cm titanium tip. The vesicles were annealed at 313 K for 30 min and centrifuged for 90 min at 48 000*g*; final samples were prepared by adding the vesicles to a stock solution of the dye in water (pH 7) to give a final dye concentration ([dye]) of 1.6×10^{-6} M (no fluorescence background or scatter from lipids).

2.3. Numerical resolution of complex fluorescence spectra

The fluorescence properties of rhodamine materials differ depending on the presence and concentration in water of lipid organizations. For a given amount of dye, different fluorescence spectra were observed depending on the concentration of DPPS and DPPG vesicles. A library of the three distinct fluorescences experimentally observed was first established by recording digitally all the spectra under standard experimental settings. The following notations were used: D^+ represents the free molecules of dye in water, D_L the dye molecules individually bound at the vesicle surface (at high vesicle concentration) and D_n the aggregated dyes on the vesicles (at $[lipid]_{agg}$). In Table 1, the fluorescence maxima of the three typical species used in the resolution treatment are given: (1) $\lambda_D{}^+$ characterizes the fluorescence spectrum of the free species ($F_D{}^+$) in water; (2) λ_{DL} characterizes the fluorescence F_{DL} of the rhodamine ligands independently bound to the lipid vesicles; (3) λ_{Dn} characterizes the fluorescence F_{Dn} of the aggregated rhodamines at the surface of the vesicles.

Complex fluorescence spectra were then resolved by mathematical analysis [16]. Theoretically, the fluorescence spectrum results from the individual emission of n chemicals numbered from 1 to n, each being characterized at each λ by its own fluorescence intensity $I_{1,\lambda}$, $I_{2,\lambda}$, etc. Since there is no energy transfer between the S_1 states of the fluorophores involved at the concentrations used (no inner filter effect), the value of the total fluorescence intensity at each λ ($I_{T,\lambda}$) was obtained through the linear combination $I_{T,\lambda} = a_1I_{1,\lambda} + a_2I_{2,\lambda} + ...$, in which a_1 and a_2 are the respective concentrations of each fluorophore in the cuvette. Numerical values of a_i can be calculated by solving a set of n of these similar $I_{T,\lambda}$ equations obtained using the different $I_{j,\lambda}$ values available from the library. However, the method was improved by summarizing all the $I_{T,\lambda}$ equations weighted by a modulating function $\phi_{j,\lambda} = I_{T,\lambda}{}^*I_{j,\lambda}$ (j running from 1 to n) resulting in a new set of more significant equations [21].

Depending on the number and the reference spectra of the library used in the treatment, different theoretical spectra were calculated and compared with the experimental data. One, two or three characteristic fluorescences ($F_D{}^+$, F_{DL}, F_{Dn}) were identified by this method and their respective participation coefficients in the complex fluorescence were quantified. Graphical and numerical estimators were calculated to verify the resolution of the composite fluorescence into its different components: (1) graphically, by plotting the weighted residuals (WR) for the composite spectra; (2) numerically, by comparing the values of the reduced chi square (χ^2) estimator derived from the variance of the distribution of WR. A good fit between an experimental result and a calculated fluorescence always results in a statistical distribution over zero of the autocorrelation function WR(λ) of the residuals and a low value of χ^2.

3. Results and discussion

Esterified R123 and R6G rhodamines, known as cationic dyes, are distinguished by their N-substituted and methylated groups. The fluorescence does not depend on the acidity of the water solution, since the hydrolysis of the ester group and the formation of a non-fluorescent photoproduct [22] only operate at very basic pH. The wavelengths of the absorption and fluorescence maxima of the R123 and R6G species in water are dependent on the pH and have been reported previously together with the pK' values [16].

3.1. Titration profiles and concentration ratios

The fluorescence spectra of rhodamine dyes are altered qualitatively by DPPG and DPPS vesicles. The anionic lipids of DPPG and DPPS shift the absorption maximum to the red (up to 10 nm) when compared with $\lambda_{Abs,max}$ in water. Similarly, the R123 and R6G fluorescences are red shifted in the presence of vesicles (from $\lambda_{Fluo,max} = 528$ nm (water) to 537 nm for R123 and from $\lambda_{Fluo,max} = 550$ nm (water) to 560 nm for R6G) (see Table 1). In addition, when using fluorescence titration to monitor quantitatively the equilibrium binding of the dyes to DPPG and DPPS vesicles, we observe, at low vesicle concentration, phenomena inconsistent with the usual

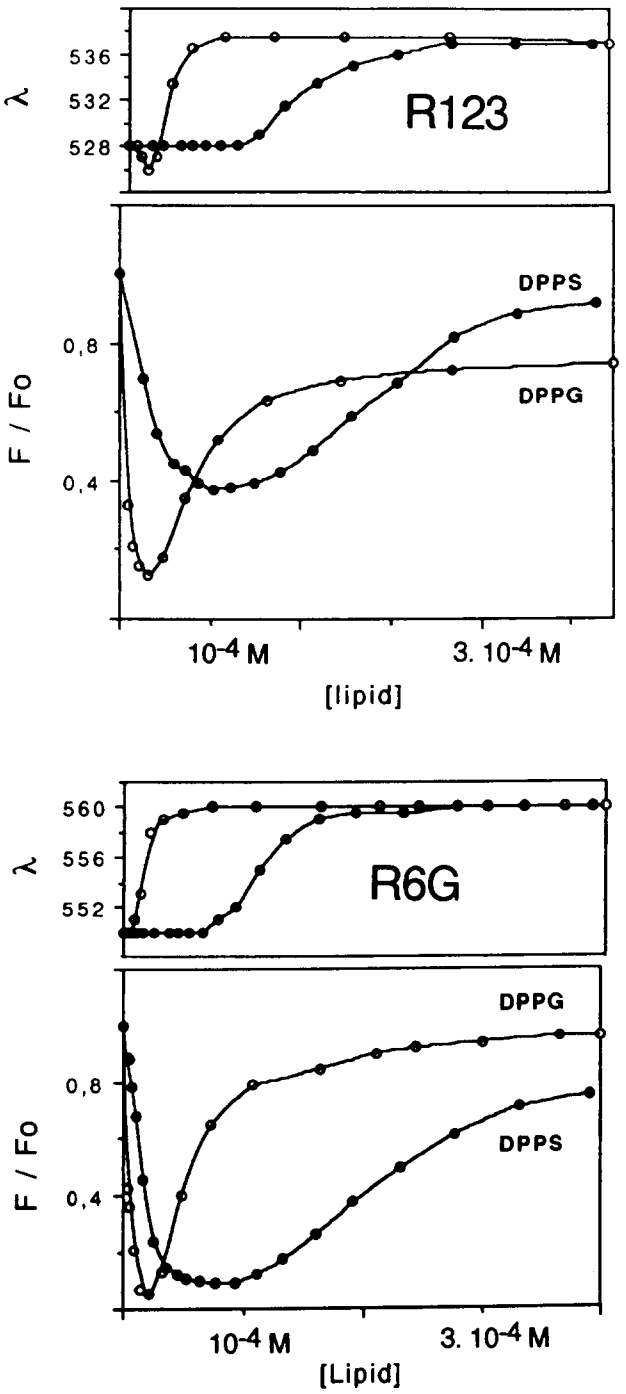

Fig. 2. Fluorometric titrations (relative intensities) and related variations in fluorescence ($\lambda_{Fluo,max}$ of R123 (a) and R6G (b) rhodamines (1.6×10^{-6} M) with DPPG and DPPS vesicles (pH 7 and $\lambda_{Exc}=480$ nm).

binding equilibria encountered in Scatchard plots. For both dyes (commonly denoted as D), there is a variation in F/F_0 on addition of DPPS and DPPG vesicles [12]. The titration profiles of F/F_0 vs. [lipid] show [13] that the intensity decrease starts at low [ves]/[D] ratios, i.e. [D]/[ves] > 50 with DPPS for both dyes and [D]/[ves] > 150 (R123) or 240 (R6G) with DPPG (Figs. 2(a) and 2(b)) (assuming a mean value of 3000 lipids per vesicle and $[D]=1.6\times10^{-6}$ M). The dyes are increasingly aggregated at the vesicle interface with an increase in [lipid] until the minimum intensity (or maximum of aggregation) is reached for $[lipid]_{agg}$. These values of $[D]/[ves]_{agg}$ (48 (R123) and 53 (R6G) with DPPS and 150 (R123) and 240 (R6G) with DPPG) and $[lipid]_{agg}$ for the different lipid–dye pairs are given in Table 1. An enhancement in F/F_0 follows the dilution of the dye by phospholipid bilayers for lipid concentrations above $[lipid]_{agg}$. Binding of the dye with more vesicles ([D]/[ves] < 50) results in disaggregation of the multimers and individual compartmentalization of the dye molecules; further dilution ([D]/[ves] < 1–15) by an excess of vesicles leads to complete disaggregation of the multimers. Then, the F/F_0 values gradually increase and almost level off at unity with increasing vesicle concentration.

3.2. Fluorometric titration

Qualitatively, a progressive red shift generally results from dye titration by the vesicles. This is observed when both rhodamines are titrated with DPPS vesicles (Figs. 3(a) and 3(c)) as well as in the case of R123 in the presence of increasing amounts of DPPG vesicles (Fig. 3(d)). An analytical treatment of the fluorescence spectra was used to resolve these composite spectra into their three different components $F_D{}^+$, F_{DL} and F_{Dn}. A specific behaviour appears at high vesicle concentration when R6G is titrated with DPPG vesicles; the λ_{Dn} fluorescence of the D_n form of the aggregated R6G molecules is not significantly shifted (see Table 1 and Fig. 2(b)) compared with the λ_{DL} emission of individually bound dye (D_L) at high DPPG vesicle concentrations. This must be associated with a corresponding decrease in magnitude (without a spectral shift) of the absorbance of the D_n species compared with the D_L species at dye saturation.

Fluorescence titration performed for $[lipid] > [lipid]_{agg}$ was used to study quantitatively the equilibrium binding of the dye molecules to DPPG and DPPS vesicles. A fixed amount of dye (1.6×10^{-6} M) was titrated with increasing concentrations of sonicated lipid vesicle solution, the extent of binding being monitored by the changes observed in $\lambda_{Fluo,max}$ and intensity. According to Eq. (1), the measured fluorescence F of a fixed amount of dye at a given lipid concentration is expressed as the sum of the characteristic fluorescences $F_D{}^+$, F_{DL} and F_{Dn} of the three species (D^+, D_L and D_n) measured under identical conditions of slits, sensitivity and λ_{Exc}

$$F=a_1F_{D^+}+a_2F_{D_L}+a_3F_{D_n} \quad (1)$$

Using the resolution method, the complex fluorescence F was resolved into its different components; the treatment provides the a_i participations of these different components for various [lipid] values, allowing the numerical values of the dye concentrations, $[D^+]$, $[D_n]$ and $[D_L]$, to be calculated. An example of the resolution of the fluorescence of R123 in DPPG vesicles at $[lipid]=4\times10^{-5}$ M is presented in Fig. 4. Titration of the dye solutions with vesicles (Figs. 2 and 3) reveals an increase in the magnitude of the fluores-

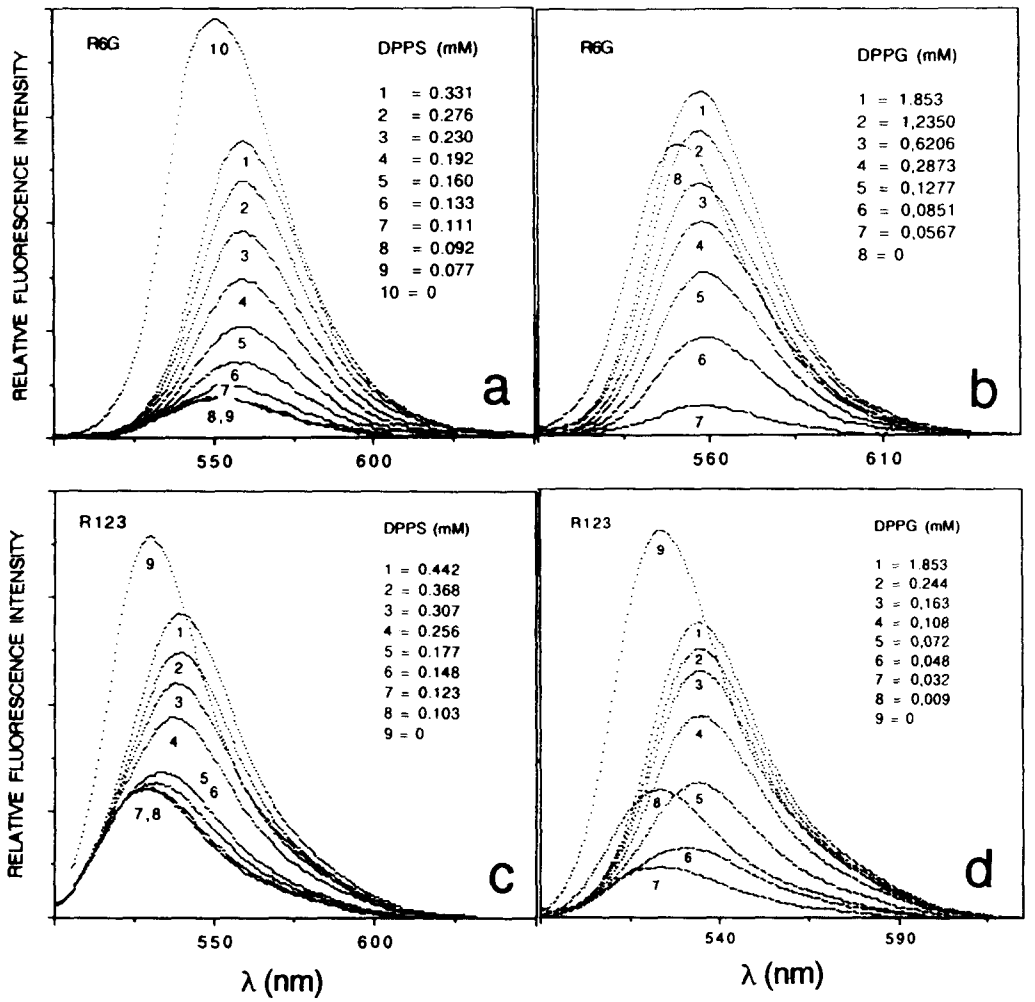

Fig. 3. Some typical fluorescence spectra of R123 and R6G dyes (1.6×10^{-6} M) in aqueous solutions (pH 7, $\lambda_{Exc}=480$ nm) and in the presence of various concentrations of DPPG and DPPS lipids (in mM).

cence change due to the vesicles ($\lambda_{Fluo,max}$ and intensity) as the [D]/[ves] ratio decreases. As has been frequently observed, this indicates that the vesicles are progressively saturated with dye through a succession of multiple equilibria between the ligands and the vesicles.

3.3. The quantitative interaction model

We wish to find, in terms of the known or measurable quantities of the total dye concentration and the total lipid concentration, the respective concentrations of the D^+, D_n and D_L forms. The statistical framework which enables us to treat and gain insight into the features of ligand interactions at equilibrium is well documented [23]. Similar to organized macrosystems, negatively charged vesicles of DPPG and DPPS possess a number of sites for interaction with R123 and R6G ligands. Such interaction involves the reversible binding of the dyes to the lipids of the vesicles in a multiple equilibria process. Theoretically, we may write for each equilibrium [24] the successive (i) individual reactions and corresponding association constants of a cooperative stepwise

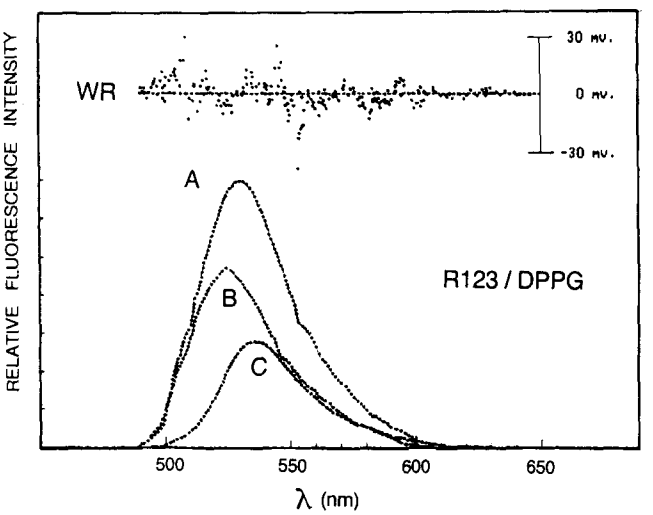

Fig. 4. Resolution patterns of the fluorescence spectrum of R123 (1.6×10^{-6} M) in the presence of [DPPG] = 4×10^{-5} M (curve A). The composite spectrum A is resolved into a 64% participation of the D_n aggregated form (curve B) and a 36% participation of the D_L species bound to the lipids (curve C). Superimposed over the fluorescence curves is the autocorrelation function WR of the residuals.

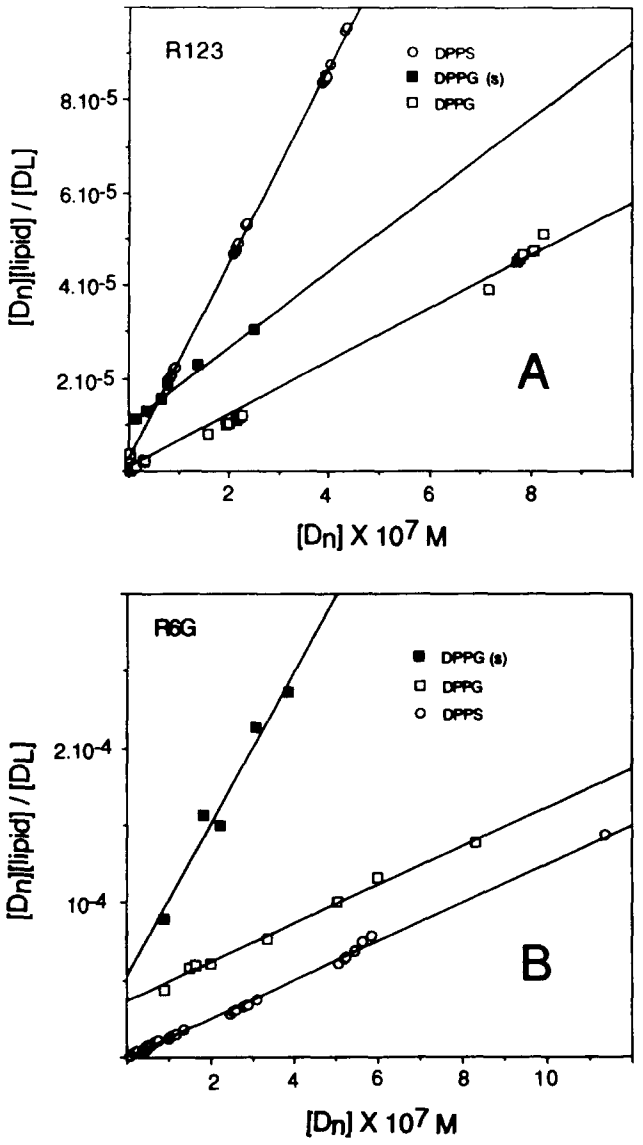

Fig. 5. Scatchard plots of $[D_n][lipid]/[D_L]$ vs. $[D_n]$ for the binding of R123 (A) and R6G (B) dyes with DPPG and DPPS phospholipid vesicles. $[D_n]$, $[D_L]$ and $\bar{n}$ represent the concentration of the aggregated species, the concentration of the bound dye and the average number of binding sites per lipid molecule respectively. Open symbols refer to the Scatchard plots (DPPG) obtained at low [ves] from the resolution method, and filled symbols represent the Scatchard plots obtained directly at high [DPPG] from the ratios of the fluorescence surfaces (see text).

association model. There will be $n!(n-i)!i!$ ways of arranging the i occupied and $(n-i)$ unoccupied sites for the lipids; however, since the number of these equilibria is indefinite, it is neither experimentally possible nor desirable to determine the concentrations of the individual species in such an equilibrium mixture. Rather, a simple description of the system can be obtained if the sites are identical and independent [25]. Thus a reasonable description of the dye–vesicle interaction is a reversible binding mechanism possessing a discrete number of binding sites. Each site has the same affinity for the ligand, and the occupation of one site has no effect on the binding to another site (identical and independent site model). The increase in D_L binding as a function of [lipid] is thus described by the simple equilibrium

$$D_n + L \overset{K_D}{\rightleftharpoons} D_L \quad (2)$$

where L represents the equivalent binding site per lipid molecule, D_n is the aggregated form of the dye on the vesicles and $K_D = [D_L]/[L][D_n]$ is the apparent equilibrium binding constant. The term "binding site", while usually reserved to describe the saturable interaction of ligands with structural pockets of enzymes or proteins [26], does not imply a specific interaction; instead, it is used as a convenient mathematical idea to set a limit to the number of dye molecules that can bind to a single vesicle, since saturation of lipid membranes by hydrophobic ions has been reported frequently [27].

The total concentration of sites $[L]_T$ is expressed as

$$[L]_T = [L] + [D_L] = \bar{n}[lipid] \quad (3)$$

where $\bar{n}$ represents the average number of equivalent binding sites per lipid molecule. To express the extend of binding, the expression $[D_n][lipid]/[D_L]$ is plotted vs. $[D_n]$ (Eq. (4))

$$[D_n][lipid]/[D_L] = 1/\bar{n}K_D + [D_n]/\bar{n} \quad (4)$$

Straight lines result from the titration of R123 and R6G dyes with DPPG and DPPS lipid vesicles (Fig. 5) in these Scatchard plots.

Corresponding n and K_D values are given in Table 2, where n is the number of sites per vesicle ($n = 300\bar{n}$), and were deduced from the slopes and intercepts obtained in linear least-squares fits. In agreement with observations for comparable molecules [28], our results are consistent with the formation in the S_0 state of D_n non-fluorescent self-aggregates at the interface of DPPG and DPPS vesicles. Both DPPS and DPPG systems provide microdomains for the favoured aggregation of R6G and R123, but the aggregation characteristics differ depending on the dye–lipid pairs and noteworthy differences are observed in the numerical values of n.

With DPPS, values of $n = 14$ (R123) and $n = 24$ (R6G) are associated with typical red shifts of $\lambda_{Fluo,max}$ on titration by vesicles. The resolution treatment and use of Eq. (4) allow these values of n (Table 2) to be determined; they agree with

Table 2
The average number n of equivalent binding sites per vesicle and the corresponding association constant K_D of ligands per lipid molecule (Eq. (2))

Vesicle	R123		R6G	
	n	K_D (M)	n	K_D (M)
DPPG	36 [b]	7.95×10^6	6 [b]	9.34×10^6
	53 [a]	6.43×10^6	24 [a]	3.43×10^6
DPPS	14	7.83×10^7	24	2.02×10^9

[a] Values measured directly at low [ves] by fluorescence intensities or fluorescence area ratios.

[b] Values determined at high [ves] through the resolution method of the fluorescence spectra.

the respective ratios ($[D]/[ves]_{agg} \simeq 50$ and $[D]/[ves]_L < 10$–14) given in Table 1.

Titration with DPPG vesicles gives two kinds of n values (denoted n^a and n^b) depending on the range of lipid concentrations used in the experiment. At low vesicle concentrations, $[D]/[ves] > 56$ (R6G) and 67 (R123), the fluorescence resolution is difficult, but still possible, since there are variations in the intensity, shape and $\lambda_{Fluo,max}$ of the fluorescence spectra as a function of [ves]; average numbers n^a of binding sites of 53 for R123 and 24 for R6G are determined. At high vesicle concentrations, $[D]/[ves] < 56$ (R6G) and 67 (R123), neither a shift in $\lambda_{Fluo,max}$ nor a change in the shape of the fluorescence spectra can be detected as a function of increasing [lipid], only a change in the fluorescence intensity. Consequently, average numbers $n^b = 36$ (R123) and $n^b = 6$ (R6G) of the second type of sites are measured directly from the fluorescence intensities or area ratios. These values agree with the concentration ratios [D]/[ves] given in Table 1.

At this level of study, the precise location and binding mechanism vs. aggregation of the rhodamine ligands to the vesicles are not yet completely understood; these questions are beyond the scope of this work, but a recent investigation has given some important insights into the complex interactions of membrane permeable hydrophobic ions with lipid vesicles [29]. When two Scatchard plots are experimentally observed, as encountered in the dye titration by DPPG vesicles, this may indicate the presence of two classes of binding site for the dye in the membrane with different K_D values. Moreover, when the variation is slowly progressive, an alternative explanation may be that the magnitude of the apparent association constant varies as more ion binds due to electrostatic effects. Similar to esterified rhodamines, other cationic amphipaths, especially those known to self-associate in aqueous solution, may develop such electrostatic interactions, ligand self-association and S_0 stacking in microdomains of negatively charged phospholipid vesicles; this may be of potential interest for the study of fractal dynamics of fluorescence energy transfer [30] and electrostatic stabilization in biomembranes.

Acknowledgments

This work was supported by grant CRE-920912 of INSERM and by the Comité des Pyrénées Orientales de la Ligue Nationale Française Contre le Cancer.

References

[1] R. Pottier and J.C. Kennedy, *J. Photochem. Photobiol. B: Biol., 8* (1990) 1.
[2] J. Miyazaki, K. Hideg and D. Marsh, *Biochim. Biophys. Acta, 1103* (1992) 62.
[3] J. Moan and S. Sommer, *Photochem. Photobiol., 40* (1984) 631; A. Blum and I.I. Grossweiner, *Photochem. Photobiol., 41* (1985) 27.
[4] A. Seret and A. van de Vorst, *J. Photochem. Photobiol. B: Biol., 17* (1993) 47; M. Hoebeke, E. Gandin, J. Decuyer and A. van de Vorst, *J. Photochem. Photobiol. A: Chem., 35* (1986) 245; J.J. Dougherty, *Photochem. Photobiol., 43* (1986) 104; J.R. Kanofsky, *Photochem. Photobiol., 53* (1991) 93.
[5] J. Moan, *Photochem. Photobiol., 43* (1986) 681.
[6] N. Mataga and M. Koizumi, *Bull. Chem. Soc. Jpn., 27* (1954) 197; M. Koizumi and N. Mataga, *Bull. Chem. Soc. Jpn., 26* (1953) 115.
[7] T. Handa, C. Ichibashi, I. Yamamoto and M. Nakagaki, *Bull. Chem. Soc. Jpn., 56* (1983) 2548.
[8] R.P. Haugland, *Handbook of Fluorescent Probes and Research Chemicals*, Molecular Probes Inc., Eugene, OR, 1992–1994.
[9] V.K. Kelkar, B.S. Valanlikar, J.T. Kunjappu and C. Manohar, *Photochem. Photobiol., 52* (1990) 717; O. Valdes-Aguilera and D.C. Neckers, *Acc. Chem. Res., 22* (1989) 171.
[10] R.K. Emaus, R. Grunwald and J.J. Lemasters, *Biochim. Biophys. Acta, 850* (1986) 436.
[11] J. Lengyel, J. Krtil, N. Rez and V. Kuban, *Nukleon, 3* (1989) 12; H. Sato, M. Kawasaki, K. Kasatani, N. Nakashima and K. Yoshihara, *Bull. Chem. Soc. Jpn., 56* (1983) 3588.
[12] R.C. Kapoor, *J. Indian Chem. Soc., 63* (1986) 541; E. De Vendittis, G. Palumbo, G. Parlato and V. Bocchini, *Anal. Biochem., 115* (1981) 278; V.N. Mishra, *Acta Chim. Hung., 116* (1984) 5; T. Ban, K. Kasatani, M. Kawasaki and H. Sato, *Photochem. Photobiol., 37* (1983) 131.
[13] M. Deumié and M. El Baraka, *J. Photochem. Photobiol. A: Chem., 74* (1993) 255.
[14] J.R. Bunting, T.Y. Phan, E. Kamali and R.M. Dowben, *Biophys. J., 56* (1989) 979.
[15] C.A. Bunton, F. Nome, F. Quina and L.S. Romsted, *Acc. Chem. Res., 24* (1991) 357.
[16] M. El Baraka, M. Deumié and P. Viallet, *J. Photochem. Photobiol. A: Chem., 62* (1991) 195.
[17] V.A. Mostonikov, G.R. Hinevitch and A.L. Shalimo, *Dokl. Akad. Nauk B. SSR, 24* (1980) 596.
[18] L.B. Chen, *Annu. Rev. Cell. Biol., 4* (1988) 155; B. Ehrenberg, V. Montana, M. Wei, J.P. Wuskell and L.M. Loew, *Biophys. J., 53* (1988) 785.
[19] R.F. Kubin and A.N. Fletcher, *J. Lumin., 27* (1982) 455; T.M. Grigor'eva, V.L. Ivanov, N. Nizamov and M.G. Kuz'min, *Dokl. Akad. Nauk SSR, 232* (1977) 1108.
[20] L.B. Johansson and A. Niemi, *J. Phys. Chem., 91* (1987) 3020.
[21] J.M. Salmon, J. Vigo and P. Viallet, *Cytometry, 9* (1988) 25.
[22] V.E. Korobov, T.D. Slovnova and A.K. Chibisov, *Zh. Prikl. Spektrosk., 26* (1977) 841.
[23] C.R. Cantor and P.R. Schimmel, *The Behavior of Biological Macromolecules*, Part III, W.H. Freeman, San Francisco, 1980.
[24] K.E. Van Holde, *Physical Chemistry*, Prentice Hall, NJ, 1971.
[25] I. Tinoco, Jr., K. Sauer and J.C. Wang, *Physical Chemistry*, Prentice Hall, NJ, 1978.
[26] M. Vermeir, N. Boens and K.P.M. Heirwegh, *Biochim. Biophys. Acta, 1107* (1992) 93.
[27] R.J. Clarke, *Biophys. Chem., 46* (1993) 131.
[28] T.G. Burke and T.R. Tritton, *Anal. Biochem., 143* (1984) 135; A.D. James and B.H. Robinson, *Adv. Mol. Relaxation Processes, 8* (1976) 287.
[29] R.J. Clarke, *Biophys. Chem., 42* (1992) 63; *39* (1991) 91.
[30] T.G. Dewey, *SPIE, 1432* (1991) 64; A.K. Bisenbaev, L.V. Levshin and A.M. Soletsky, *J. Mol. Struct., 266* (1992) 411.